

Numerical simulations of dense granular flow in a two-dimensional channel:The role of exit position

Tingwei Wang(王廷伟), Xin Li(李鑫), Qianqian Wu(武倩倩), Tengfei Jiao(矫滕菲), Xingyi Liu(刘行易), Min Sun(孙敏), Fenglan Hu(胡凤兰), Decai Huang(黄德财)

Citation: Chin. Phys. B . 2018, 27(12): 124704. **doi:** 10.1088/1674-1056/27/12/124704
Journal homepage: http://cpb.iphy.ac.cn; http://iopscience.iop.org/cpb

What follows is a list of articles you may be interested in

A numerical study of contact force in competitive evacuation

Peng Lin(林鹏), Jian Ma(马剑), You-Ling Si(司有亮), Fan-Yu Wu(吴凡雨), Guo-Yuan Wang(王国元), Jian-Yu Wang(王建宇)
Chin. Phys. B . 2017, 26(10): 104501. **doi:** 10.1088/1674-1056/26/10/104501

Ultrasound wave propagation in glass-bead packing under isotropic compression and uniaxial shear

Zhi-Gang Zhou(周志刚), Yi-Min Jiang(蒋亦民), Mei-Ying Hou(厚美瑛)
Chin. Phys. B . 2017, 26(8): 084502. **doi:** 10.1088/1674-1056/26/8/084502

Nano watermill driven by revolving charge

Zhou Xiao-Yan, Kou Jian-Long, Nie Xue-Chuan, Wu Feng-Min, Liu Yang, Lu Hang-Jun
Chin. Phys. B . 2015, 24(7): 074702. **doi:** 10.1088/1674-1056/24/7/074702

Asymmetry of the water flux induced by the deformation of a nanotube

He Jun-Xia,Lu Hang-Jun,Liu Yang,Wu Feng-Min,Nie Xue-Chuan,Zhou Xiao-Yan,Chen Yan-Yan
Chin. Phys. B . 2012, 21(5): 054703. **doi:** 10.1088/1674-1056/21/5/054703

Maturing process of solitary wave train in a step-down chain

Xia Ji-Hong,Wang Ping-Jian,Liu Chang-Song
Chin. Phys. B . 2012, 21(2): 024501. **doi:** 10.1088/1674-1056/21/2/024501

Numerical simulations of dense granular flow in a two-dimensional channel: The role of exit position*

Tingwei Wang(王廷伟), Xin Li(李鑫), Qianqian Wu(武倩倩), Tengfei Jiao(矫滕菲), Xingyi Liu(刘行易), Min Sun(孙敏), Fenglan Hu(胡凤兰), and Decai Huang(黄德财)†

Department of Applied Physics, Nanjing University of Science and Technology, Nanjing 210094, *China*

(Received 25 July 2018; revised manuscript received 19 September 2018; published online 10 November 2018)

Molecular dynamics simulations have been performed to elucidate the influence of exit position on a dense granular flow in a two-dimensional channel. The results show that the dense flow rate remains constant when the exit is far from the channel wall and increases exponentially when the exit moves close to the lateral position. Beverloo's law proves to be successful in describing the relation between the dense flow rate and the exit size for both the center and the lateral exits. Further simulated results confirm the existence of arch-like structure of contact force above the exit. The effective exit size is enlarged when the exit moves from the center to the lateral position. As compared with the granular flow of the center exit, both the vertical velocities of the grains and the flow rate increase for the lateral exit.

Keywords: granular materials, dense granular flow, molecular dynamics simulations

PACS: 47.57.Gc, 45.70.Mg, 75.40.Mg **DOI:** 10.1088/1674-1056/27/12/124704

1. Introduction

The flow of granular materials has been a research topic of extensive interest in scientific and engineering fields and is involved in many complex phenomena such as avalanches,[1–3] mixing and segregation,[4–6] and jamming.[7–9] When granular flow is confined in a silo with an exit, a typical flow state is the dense granular flow and the most important issue is how to control the flow rate.[10–12]

Contrary to normal fluid, one of the interesting features of packing granular materials is that the pressure at the bottom of silo saturates when the packing height is greater than a certain value.[13–15] The dense flow rate has been found to be independent of the packing height and many works have focused on the factors that influence the flow rate and corresponding physical mechanism.[16,17] The most widely accepted formula of the flow rate was proposed by Beverloo *et al.* in 1961.[18] According to Beverloo's law, when the mono-sized grains are discharged through an exit at the bottom of silo, the dense flow rate Q can be written as,

$$Q = C\sqrt{g}(D-kd)^{n-1/2}, \tag{1}$$

where n is the spatial dimension (*e.g.*, $n = 2$ and 3 for two- and three-dimensional exit, respectively). g is the acceleration of gravity. D and d are the diameters of the exit and the grains. C is a dimensional coefficient and may have relation with the friction coefficient and packing density of the grains. k is a geometrical factor related to the shapes of the exit and the grains. Equation (1) is derived based on dimensional analysis and physically explained by assuming an arch-like structure of contact force above the exit. In this assumption, the grains are closely compacted in the region of the arch above the exit. The grains lose their velocities in the region of the arch and then fall freely due to self-gravity below the arch. In addition, there is an annular empty area around the edge of the exit at which grains' center cannot arrive. Therefore, the effective diameter $D-kd$ of the exit must be less than the original diameter D. Thus the power of $n-1/2$ is reasonably calculated by the product of the falling velocity of the grains and corresponding cross area.

Many experimental and numerical works have been carried out to examine the validity of Beverloo's Eq. (1) and proved it to be successful.[19–22] For example, Behringer *et al.* studied the influence of grains' shapes on their flow rate.[23] They fitted the flow rates of both circular and elliptical grains by Beverloo's law, and found that the parameter k for the elliptical grains is larger than that for the circular grains. This means that the effective exit size is smaller for the elliptical than for the circular grains. In fact, experimental results have shown that elliptical grains tend to form a force arch above the exit more easily than circular grains. This leads to smaller velocities and hence reduced flow rate for the elliptical than for the circular grains, in good agreement with the prediction of Beverloo's law. Recent works have shown that the exit position is another factor that controls the flow rate of the grains.[24,25] Medina *et al.* found that the velocity oscil-

*Project supported by the National Natural Science Foundation of China (Grant No. 11574153).

†Corresponding author. E-mail: hdc@njust.edu.cn

© 2018 Chinese Physical Society and IOP Publishing Ltd

lation observed in silo with the exit located at the center is not detected when the exit is moved to the lateral position.[26] To the best of our knowledge, the influence of exit position on dense flow rate has not been thoroughly explored, and a more detailed study on this issue would be useful for a better understanding of the flow of granular materials.

In this work, molecular dynamics simulations have been performed to elucidate the influence of exit position on dense granular flow in a two-dimensional (2D) channel. We describe our simulation model and method in Section 2. The flow rate in any subregion of the exit is defined by calculating corresponding packing density and the velocity of the grains. In Section 3, we explore the relation between the flow rate and the exit position and simulate two special systems, *e.g.*, the exits located at the center and the lateral positions, to test the validity of Beverloo's law. The influence of the exit position on contact force between grains, flow velocity and packing fraction are quantitatively analyzed. Our major results are summarized in the conclusion.

2. Simulation model

The influence of the exit position on the dense granular flow in a quasi-two-dimensional channel has been explored by molecular dynamics (MD) simulations. The channel was chosen to be $H = 400.0$ mm in height, $W = 80$ mm in width, and $T = 2.0$ mm in thickness. The exit is located at the height of $H_{\mathrm{E}} = 25.0$mm by using two plane baffles. The widths of the left and the right baffles are W_1 and W_2, respectively. In the present work, the exit position is an adjustable parameter. The exit is situated at the center of the channel (Fig. 1(a) inset) when $W_1 = W_2$, and the lateral exit corresponds to $W_2 = 0$ (Fig. 1(b) inset). All of the grains have a circular shape and their thickness is identical to that of the channel.

The discrete element method was used in MD simulations to describe the motion of each particle. In each simulation time step, the positions and velocities of particles were updated by integrating Newton's second law of motion. The effective gravity was set to be $g\sin 15^\circ$ which has been used in our previous studies.[27,28] g is the gravitational acceleration. Both the translational motion in the 2D channel plane and the rotational motion about an axis in the direction perpendicular to the channel plane were considered in the simulations. The force between two contacting particles was calculated in the normal and tangential directions, where the normal interaction is described by the Kuwabara–Kono model[29,30]

$$F_{ij}^{n} = -k_n {\xi_{ij}}^{3/2} - \eta_n {\xi_{ij}}^{1/2} V_{ij}^{n}, \tag{2}$$

and the tangential component is taken to be the minor of the tangential force with a memory effect and the dynamic frictional force.

$$F_{ij}^{\tau} = -\min(k_t \zeta_{ij}, \mu F_{ij}^{n}). \tag{3}$$

In Eqs. (2) and (3), the subscripts i and j are the indexes of the particles. $\xi_{ij} = \max(0, d_{ij} - |\boldsymbol{x}_i - \boldsymbol{x}_j|)$ is the overlap of the contacting particles i and j, and d is the sum of radii of the contacting particles r_i and r_j. ζ_{ij} denotes the displacement in the tangential direction from the initial time t_0 when the contact is first established to the current time t, *i.e.*,

$$\zeta_{ij}(t) = \int_{t_0}^{t} v_{\tau}(t')\,\mathrm{d}t'$$

and

$$\boldsymbol{V}_{ij} = V_{ij}^{n}\boldsymbol{e}_n + V_{ij}^{\tau}\boldsymbol{e}_{\tau}$$

is the relative velocity of two particles. The indexes n and τ represent the normal and tangential directions at the contact point, respectively. k_n, k_t, and η_n characterize the normal and tangential stiffnesses and damping of the granular materials and are related to the collision time t_n and the masses of contacting particles m_i and m_j. The detailed values can be calculated as follows:

$$k_n = \frac{4}{3}\frac{Y_i Y_j}{Y_i + Y_j}\sqrt{\frac{R_i R_j}{R_i + R_j}},$$

$$k_t = \frac{2}{7}\frac{m_i m_j}{m_i + m_j}\left(\frac{\pi}{t_n}\right)^2, \qquad Y = \frac{E}{1-\nu^2},$$

$$t_n = 3.21\left[\frac{m_i m_j}{k_n(m_i + m_j)}\right]^{2/5}(V_{ij}^{n})^{-1/5},$$

where E is the Young's modulus and ν is the Poisson ratio. The coefficient of dynamic friction μ is fixed in our MD simulations. The collisions between the particles and the channel wall are treated as particle–particle collisions, except that the wall has an infinite mass and an infinite diameter. The parameters of the grain materials are listed in Table 1.

Table 1. The parameters of the grain materials.

Quantity	Symbol	Value
Diameter/mm	d	2.0
Density/(kg/m^3)	ρ	2500
Young's modulus/GPa	E	1.0
Poisson's ratio	ν	0.3
Normal damping coefficient/(Nm$^{3/2}\cdot$s)	η_n	30.0
Dynamic frictional coefficient	μ	0.5
Simulation time-step/s	dt	10^{-6}

Two simulation conditions were performed in our MD simulations. One is the non-periodical condition. Under this condition, the exit was first plugged up by placing a plane baffle. The grains randomly entered the channel from the top of

the channel and accumulate above the baffle. When the number of grains in the channel amounted to 8000, the packing height of the grains is about $175d$. The inflow grains stopped and the baffle on the exit was drawn out. The grains started to flow out through the exit. Under this condition, no more grains flowed into the channel and the channel would be empty in the end. The other is the periodical condition, under which the grains would re-enter the channel from the top when they passed through the bottom of the channel. The packing grains can be kept at the height of $H = 125d$ when the number of grains is $N = 5992$. The channel is divided into rectangular subregions by using $0.3d \times 1.0d$ in the x and y directions, respectively. In each rectangular subregion, the instantaneous flow rate can be directly calculated as follows:

$$q = \frac{\sum_i \phi_i v_{yi}}{d}, \tag{4}$$

where q is the local flow rate and $\sum_i$ represents the summation over all particles intersecting with the rectangular subregion. ϕ_i is the cross section of i-th particle with the rectangular subregion and v_{yi} is the velocity of the grains in the y direction. So the flow rate Q at the exit can be obtained by summing q along the x direction of the exit.

3. Results and discussions

Figure 1(a) is a comparison of the simulated results under two flow conditions when the exit is located at the center of channel. At the beginning of simulation, the flow rate increases quickly and gets to a steady value for both flow conditions ($Q = 1036.42$ s^{-1}). Then, under the non-periodical condition, the flow rate starts to decrease continuously when the packing height of the grains is less than a certain height. In contrast, the flow rate fluctuates around a fixed value under the periodical condition.

Figure 1(b) shows similar results when the exit is shifted to the lateral position. In the periodical condition, the flow rate can remain constant ($Q = 1266.16$ s^{-1}) throughout the whole simulation time. This method is adopted in the simulations to perform long-time statistics.

Figure 2(a) shows the flow rate as a function of exit position with four exit sizes $D/d = 6.0$, 8.0, 10.0, and 12.0, respectively. When the exit is placed at the center of channel, the corresponding flow rates Q_0 are emphasized by solid symbols. We can see that the flow rates fluctuate around a constant value for each exit size when the exit is far from the channel wall, $W_2/d \gg 0$. The averaged flow rates are shown in dashed lines, $Q = 389.73$, 684.91, 1033.81, and 1422.45 s^{-1}, respectively. In contrast, the flow rate increases monotonically as the exit approaches the right channel wall, $W_2/d \to 0$. On the other hand, the profiles of all curves in Fig. 2(a) seem to share similar features. In Fig. 2(b), the reduced flow rates ($\gamma = Q/Q_0$) versus the scaled exit position ($\chi_E = 2W_2/(W-D)$) for all cases in Fig. 2(a) are well collapsed into a single curve described by the following equation,

$$Q = Q_0(1 + \alpha e^{-\beta \chi_E}), \tag{5}$$

where $\alpha = 0.27 \pm 0.035$ and $\beta = 19.08 \pm 2.58$ are the fitting parameters. When the exit is far from the channel wall, $\chi_E \to 1.0$, the channel wall has no effect on the flow properties, and the flow rate is independent of the exit position, $\gamma = 1$. When the exit is shifted toward the channel wall, $\chi_E \to 0$, the effect of the wall on the flow rate becomes stronger. In the condition of $\chi_E = 0$, the influence of the right baffle on flow rate disappears completely and the channel wall plays the dominant role.

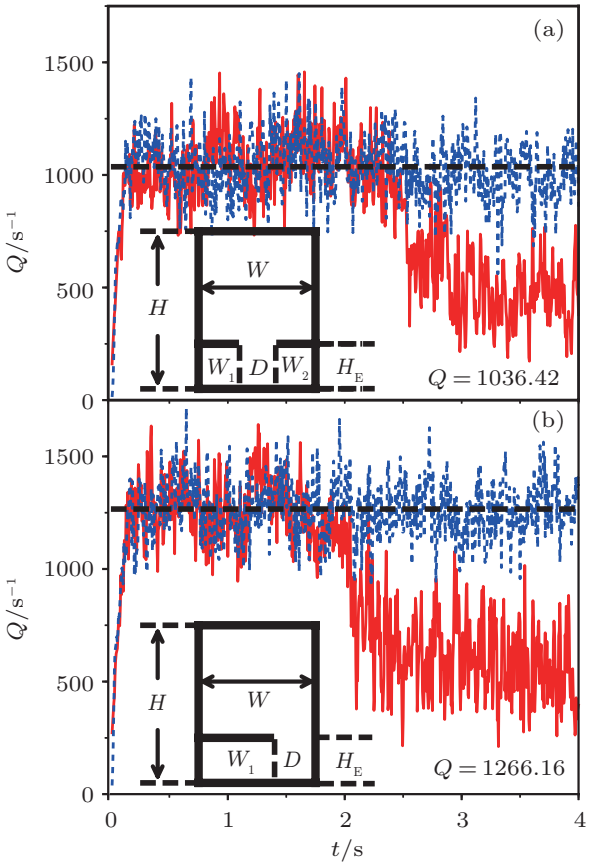


Fig. 1. (color online) The flow rate as a function of time for (a) center exit and (b) lateral exit. The red solid and blue dotted lines stand for non-periodical and periodical conditions, respectively. The dashed lines denote the averaged flow rates. The insets are the sketches of simulation setups.

In Fig. 2(a), there is an obvious abrupt increase in the flow rate of $W_2/d = 0$ over that of $W_2/d = 1.0$. Taking the case of the exit $D/d = 12.0$ as an example, the flow rate is $Q = 1730.75$ s^{-1} for the lateral exit $W_2/d = 0$ and it becomes 1422.45 s^{-1} as the exit is close to the center $W_2/d \to 1.0$. The jump between the flow rates for the center and the lateral exits is marked in Fig. 2(a).

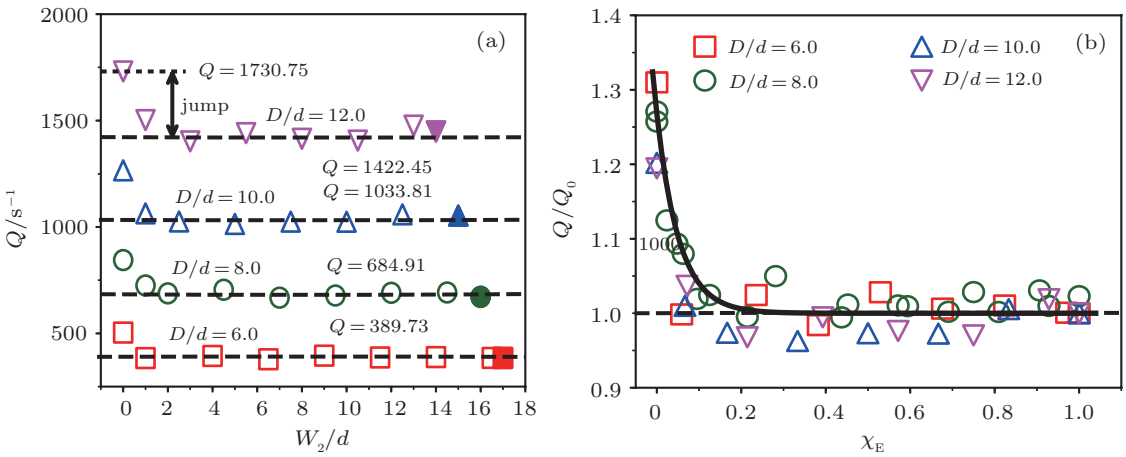


Fig. 2. (color online) (a) Flow rate Q as a function of exit position with four exit sizes $D/d = 6.0$, 8.0, 10.0, and 12.0, respectively. The dashed lines stand for the average flow rates. (b) Relationship between the scaled flow rate and the scaled exit position. The solid line is fitted by using Eq. (5). The dashed line is a guide for the eye.

To examine the validity of Beverloo's law, figure 3 plots the dependence of the flow rate on the exit size for the center and the lateral exits. Two kinds of channels with widths $W/d = 40.0$ and 50.0 have been simulated. The good agreement between our simulated results and the theoretical curves clearly indicates that Beverloo's law holds well. The relationship between the flow rate and the exit size follows the power of $3/2$, which implies the free-falling mechanism may govern the flow properties. The fitting parameters C and k are 28.00 and 1.82 for the center exit, and 31.65 and 1.43 for the lateral exit. In the simulations, the frictional coefficients between the grains and between the grain and the wall were fixed. As the exit is moved from the center to the lateral position, an increase in C corresponds to a higher packing density. On the other hand, the decrease in k means the decrease in the annular section, and a larger effective exit size is obtained.

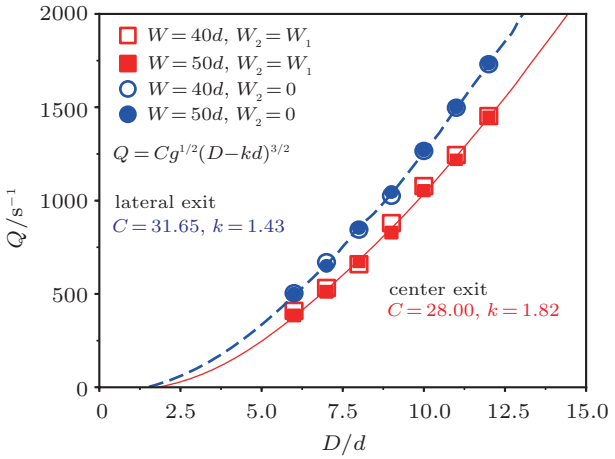


Fig. 3. (color online) Simulated results of flow rate as a function of exit size. The squares and circles stand for the center and lateral exits, respectively. The open and solid symbols correspond to the channels with width $W/d = 40.0$ and 50.0. The solid and dashed lines are obtained by using Beverloo's equation.

Figure 4 illustrates the distribution of time-averaged contact force between grains for the exits at the center and lateral positions. The exit size is fixed at $D/d = 10.0$. In Fig. 4(a), a semi-circular structure of force arch can be clearly observed above the exit. Under the force arch, contact force is barely detected which suggests the grains lose touch with each other. And thus the grains flow out through the exit just due to self-gravity. In Fig. 4(b), we can see that the contact force above the exit is also stronger than that in the region of the exit. The free-falling region around the exit are enlarged in comparison with that in Fig. 4(a). This extension leads to an increase in the effective exit size. The flow rate for the lateral exit is thus larger than that for the center exit.

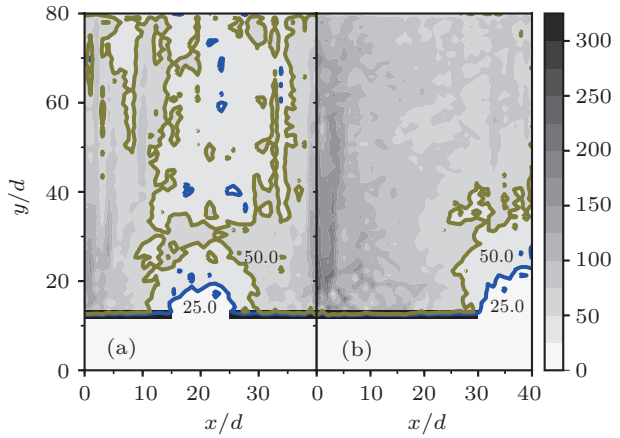


Fig. 4. (color online) Comparison of the contact force between grains for (a) the center exit and (b) the lateral exit. The exit size is set to $D/d = 10.0$. The darker color indicates higher contact force in units of the gravitational force of one grain. The blue (25.0) and olive (50.0) lines are marked to emphasize the profile of arch above the exit.

The velocity of the grains and the packing density are two key quantities that contribute to the flow rate. To make a further comparison, figure 5 shows the time-averaged velocity v_y of the grains, packing density ϕ, and flow rate q in the subregions of the exit. Here we have chosen the center of exit as the

origin of the coordinate system. The conditions are the same as those in Fig. 4. The simulated results are in agreement with the characteristics of free-falling motion. A symmetrical profile is observed when the exit is placed at the center of channel. As the exit is shifted to the right lateral position of the channel, the velocity of the grains almost collapses together for the regions close to the left of exit. The velocity of the grains for the right region of the exit is expected to be larger than that for the left of the exit. These features are consistent with those observed in Fig. 4. The increase in the effective exit size leads to increase in the velocity of the grains. Similarly, the packing density keeps symmetrical for the case of the center exit. As the exit is moved to the lateral position, the packing density for the right of the exit exceeds that for the left of the exit. It is worth noticing that there appear a series of fluctuations in the regions close to the edge of the exit. This fluctuation is more evident for the lateral exit.

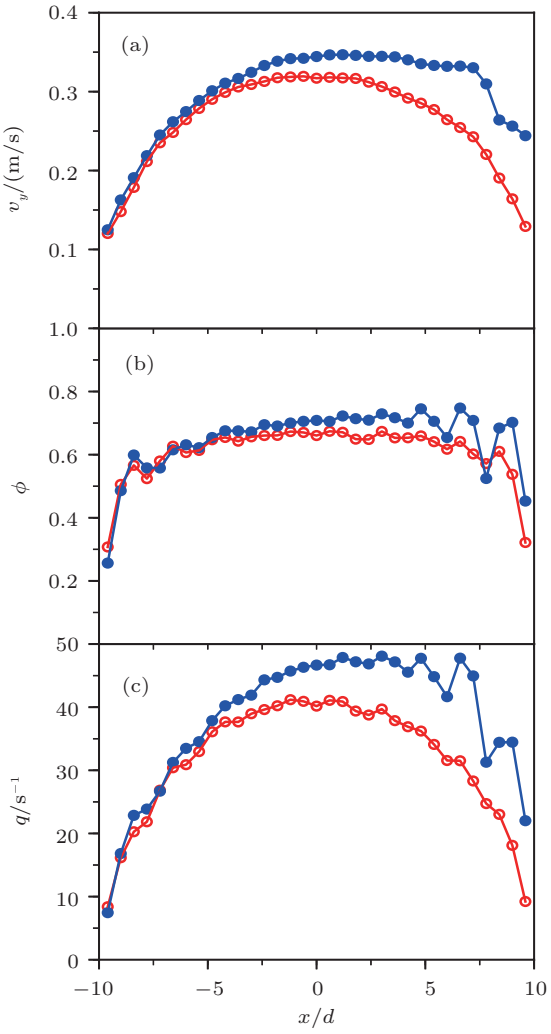


Fig. 5. (color online) Comparison of (a) the velocity of the grains v_y, (b) packing density ϕ, and (c) flow rate q for the center exit (red open circles) and the lateral exit (blue solid circles). The same simulation parameters are used as that in Fig. 4. The origin of the coordinate system is located at the center of the exit. The lines are guides for the eye.

Figure 5(c) shows the distribution of the flow rate at the subregions of the exit. Compared to the distributions in Figs. 5(a) and 5(b), the symmetry is maintained for the case of the center exit but is broken for the case of the lateral exit. Furthermore, the fluctuation in the packing density plays the dominant role in the fluctuation of the flow rate, especially for the subregions close to the channel wall.

4. Conclusions

In this work, the influence of the exit position on the dense granular flow in a 2D channel has been investigated by numerical simulations. The results show that the dense flow rate remains constant when the exit is far from the channel wall and the dense flow rate has an abrupt increase as the exit is moved to the lateral position of the channel. The dependence of the dense flow rate on the scaled exit position can be described by the function $Q = Q_0(1 + \alpha \mathrm{e}^{-\beta \chi_{\mathrm{E}}})$.

Our simulated results demonstrate that Beverloo's law is successful in describing the relation between the flow rate and the exit size when the exit is placed at the center and the lateral positions of the channel. The time-averaged contact force between the grains indicates the existence of a force arch above the exit. Compared to the case with the exit at the center position, the effective exit size is enlarged when the exit is move to the lateral position. Further simulations show that the velocity of the grains, the packing density and the flow rate are increased for the subregions close to the lateral wall. Generally, the results presented in this paper have potential industrial and theoretical implications considering the importance of processing the flow of granular materials.

References

[1] Jaeger H M, Nagel S R and Behringer R P 1996 *Rev. Mod. Phys.* **68** 1259
[2] Bursik M, Patra A, Pitman E B, Nichita C, Macias J L, Saucedo R and Girina O 2005 *Rep. Prog. Phys.* **68** 271
[3] Denisov D V, Lörinca K A, Uhi J T, Dahmen K A and Schall P 2016 *Nat. Commum.* **7** 10641
[4] Huang D C , Lu M, Sen S, Sun M, Feng Y D and Yang A N 2013 *Eur. Phys. J. E* **36** 41
[5] Shi Q, Sun G, Hou M Y and Lu K Q 2007 *Phys. Rev. E* **75** 061302
[6] Wang W G, Zhou Z Z, Zong J and Hou M Y 2017 *Chin. Phys. B* **26** 044501
[7] Thomas C C and Durain D J 2015 *Phys. Rev. Lett.* **114** 178001
[8] Gella D, Maza D, Zuriguel I, Ashour A, Arévalo R and Stannarius R 2017 *Phys. Rev. Fluids* **2** 084304
[9] To K W, Lai P K and Pak H K 2000 *Phys. Rev. Lett.* **86** 71
[10] Fortterre Y and Pouliquen O 2008 *Ann. Rev. Fluid Mech.* **40** 1
[11] Hou M, Chen W, Zhang T, Lu K Q and Chan C K 2003 *Phys. Rev. Lett.* **91** 204301
[12] Mathews J C and Wu W 2016 *Powder Technol.* **293** 3
[13] Perlta J P, Aguirre M A, Géminard J C and Pugnalonis L A 2017 *Powder Technol.* **311** 265
[14] Vanel L and Clément E 1999 *Eur. Phys. J. B* **11** 525
[15] Qadir A, Shi Q F, Liang X W and Sun G 2010 *Chin. Phys. B* **19** 034601

[16] Rubio-largo S M, Janda A, Maza D, Zuriguel I and Hidalgo R C 2015 *Phys. Rev. Lett.* **1**14 238002
[17] Zhang X Z, Zhang S, Yang G H, Lin P, Tian Y, Wan J F and Yang L 2016 *Phys. Lett. A* **3**80 1301
[18] Beverloo W A, Leniger H A and van de Velde J 1961 *Chem. Eng. Sci.* **1**5 260
[19] Janda A, Zuriguel I and Maza D 2012 *Phys. Rev. Lett.* **1**08 248001
[20] Benyamine M, Djermane M, Dalloz-Dubrujeaud B and Aussillous P 2014 *Phys. Rev. E* **9**0 032201
[21] Zhou Y, Ruyer P and Aussillous P 2015 *Phys. Rev. E* **9**2 062204
[22] Wang Y, Lu Y and Ooi J Y 2015 *Powder Technol.* **2**82 43
[23] Tang J and Behringer R P 2016 *Euro Phys. Lett.* **1**14 34002
[24] Xu C, Wang F L, Wang L P, Qi X S, Shi Q F, Li L S and Zheng N 2018 *Powder Technol.* **3**28 7
[25] Serrano D A, Medina A, Chanvarria R, Pliego M and Klapp J 2015 *Powder Technol.* **2**86 438
[26] Medina A, Andrade J, Córdova J A and Treviño C 2000 *Phys. Lett. A* **2**73 109
[27] Huang D C, Sun G and Lu K Q 2006 *Phys. Rev. E* **7**4 061306
[28] Huang D C, Sun G and Lu K Q 2011 *Phys. Lett. A* **3**75 3375
[29] Kuwabara G and Kono K 1987 *Jpn. J. Appl. Phys.* **2**6 1230
[30] Schäfer J, Dippel S and Wolf D E 1996 *J. Phys. I* **6** 5